Iranian Journal of Basic Medical Sciences
ijbms.mums.ac.ir

Fabrication of a five-layer wound dressing containing chitosan-LL37 peptide for the treatment of EB wounds and deep exudate patients

Morteza Rabiei [1], Mehrdad Moosazadeh Moghaddam [2], Hossein Derakhshankhah [3], Ramezan Ali Taheri [1]*

[1] Nanobiotechnology Research Center, New Health Technologies Institute, Baqiyatallah University of Medical Sciences, Tehran, Iran
[2] Tissue Engineering and Regenerative Medicine Research Center, New Health Technologies Institute, Baqiyatallah University of Medical Sciences, Tehran, Iran
[3] Pharmaceutical Sciences Research Center, Health Institute, Kermanshah University of Medical Sciences, Kermanshah, Iran

ARTICLE INFO

Article type:
Original

Article history:
Received: Jan 29, 2026
Accepted: May 19, 2026

Keywords:
Antibacterial peptide
Chitosan
Epidermolysis bullosa (EB)
PDMS
Wound healing

ABSTRACT

Objective(s): This study aimed to develop and evaluate a multifunctional five-layer wound dressing that meets essential requirements for effective wound healing, including exudate absorption, antimicrobial activity, moisture retention, gas exchange, and non-damaging adhesion. The specific objective was to assess the antibacterial efficacy, biocompatibility, and wound-healing performance of a dressing incorporating chitosan–LL37 nanoparticles (CS-LL37 NPs).

Materials and Methods: A five-layer wound dressing was fabricated, consisting of a silicone adhesive layer, a polyurethane (PU) foam layer embedded with CS-LL37 NPs, a polypropylene diffusion layer, a cellulose-based retention layer, and a breathable, waterproof backing layer. The CS-LL37 NPs were incorporated into the PU layer, and their antibacterial activity and cytotoxicity were evaluated *in vitro*. The dressing's wound-healing performance, with and without CS-LL37 NPs, was assessed *in vivo* in a female Wistar rat model and compared with that of a commercial dressing (Mepilex Border).

Results: The developed five-layer dressing demonstrated effective exudate management, antimicrobial activity, and favorable healing conditions. *In vivo* results showed wound closure rates and histological outcomes comparable to those of the commercial dressing. The inclusion of CS-LL37 NPs enhanced antibacterial performance without inducing significant cytotoxicity, indicating good biocompatibility.

Conclusion: The prepared five-layer wound dressing exhibited healing performance comparable to a commercially available product. The incorporation of CS-LL37 nanoparticles showed significant potential to improve treatment outcomes, particularly for exudative wounds, and may be a promising option for patients with chronic or fragile-skin conditions such as Epidermolysis Bullosa.

▶ Please cite this article as:
Rabiei M, Moosazadeh Moghaddam M, Derakhshankhah H, Taheri RA. Fabrication of a five-layer wound dressing containing chitosan-LL37 peptide for the treatment of EB wounds and deep exudate patients. Iran J Basic Med Sci 2026; 29:

Introduction

The importance of skin adhesion in wound dressings cannot be overstated. Achieving the right balance is critical to ensure that the dressing adheres effectively to the skin without causing damage during removal. Silicone-based dressings have gained significant popularity in the medical industry for their ability to address this challenge. They offer moderate adhesion, allowing secure attachment to the skin while enabling gentle removal, thereby minimizing trauma to the wound and surrounding tissues. Soft silicone has adhesive properties that remain stable over time and adapt well to uneven skin surfaces and joints. Additionally, it is non-toxic, non-allergenic, and promotes tissue regeneration, making it an ideal material for wound care. One commonly used medical-grade silicone is polydimethylsiloxane (PDMS), a versatile polymer with numerous applications in the medical field. PDMS is utilized in medical implants, wound dressings, catheters, dialysis membranes, microvalves, and more. However, in certain medical applications, it is necessary to modify PDMS to make it hydrophilic. Due to its inherent hydrophobicity, various methods have been developed to enhance its hydrophilicity and adhesion. These methods include adjusting the PDMS-to-hardener ratio, incorporating water into its composition, and blending it with polymers such as gelatin and polyethylene glycol (PEG) (1, 2). The layer following the porous layer should be capable of absorbing wound secretions by creating negative pressure. Materials such as foam, sponge, film, woven fabric, or non-woven fabric can be used for this layer. One commonly used material is PU foam, which is highly effective due to its unique properties. PU foam can swell up to 100% of its original volume, with some formulations expanding up to 800%,

***Corresponding author:** Ramezan Ali Taheri. Nanobiotechnology Research Center, New Health Technologies Institute, Baqiyatallah University of Medical Sciences, Tehran, Iran. Tel: +98-2188068924, Email: taheri@bmsu.ac.ir

while maintaining its structural integrity and strength. This layer can also be infused with antibacterial agents to prevent wound infections and promote a sterile healing environment (3). In addition, the polyurethane layer, in combination with the semi-permeable backing layer, helps maintain optimal moisture levels in the wound area while facilitating gas exchange. This dual functionality creates an ideal environment for wound healing by preventing excessive drying or maceration and ensuring proper oxygenation of the tissue (4). Polyurethane, on its own, is limited in its ability to absorb exudates due to its hydrophobic nature and lacks inherent antibacterial properties. However, these limitations can be effectively addressed by incorporating antibacterial substances or modifying the material through blending, bonding, or coating with hydrophilic polymers. Promising solutions include the addition of antibacterial peptides, antichromosensory molecules, essential oils, bacteriolytic enzymes, micro- and nanomaterial structures, and natural antimicrobial molecules and macromolecules. These modifications enhance both the exudate absorption capacity and the antibacterial efficacy of the polyurethane layer (5). Chitosan is a versatile material often used as an additive to polyurethane. Its incorporation into polyurethane can serve multiple roles, such as acting as a chain extender, cross-linking agent, or modifier to enhance mechanical properties, thermal stability, biodegradability, and antibacterial activity. The formation of hydrogen bonds between polyurethane and chitosan facilitates the uniform dispersion of chitosan within the polyurethane matrix. This interaction improves mechanical properties such as tensile strength, flexibility, and elastomeric behavior, making the composite suitable for applications like suture threads. Additionally, the urethane groups in polyurethane react with the amino (NH_2) groups of chitosan, forming strong intermolecular hydrogen bonds that further enhance the material's performance (6).

Antimicrobial peptides (AMPs) are essential components of the innate immune system. They are typically cationic, amphiphilic peptides of 50 amino acids or fewer, rich in arginine and lysine residues. One such AMP is the LL37 peptide, commonly known as Cathelicidin. This peptide is found in various cells, tissues, and bodily fluids at varying concentrations. LL37 exhibits potent antibacterial and immunomodulatory activities and plays a significant role in promoting angiogenesis and re-epithelialization during wound healing (7). Several challenges, including poor stability in biological environments, susceptibility to proteolytic digestion in bodily fluids, weak interactions with host macromolecules, and potential toxicity, limit the clinical application of the LL37 peptide. Encapsulating LL37 within nanoparticles offers a promising solution to these issues. When LL37 is encapsulated in chitosan nanoparticles, its bioavailability, stability, and sustained release are significantly improved. This approach also enables controlled pharmacokinetics, reduces toxicity, and enhances interactions with target molecules. Furthermore, chitosan nanoparticles possess inherent antibacterial and antiviral properties that synergistically enhance the antibacterial, antibiofilm, and multidrug resistance (MDR) activities of LL37 (8). Encapsulating the LL37 peptide in chitosan nanoparticles and embedding these nanoparticles within polyurethane foam can create a synergistic effect. This approach enhances peptide retention and stability, improves the physicochemical properties of the polyurethane layer, and ultimately accelerates wound healing.

The diffusion layer, the third layer of the wound dressing, facilitates the transfer of moisture from the PU foam layer to the maintenance layer. It also ensures even distribution of liquid both horizontally and vertically, preventing fluid accumulation in one area (9). The fourth layer, known as the maintenance layer, is a critical component of an ideal wound dressing. It is designed to absorb and retain large volumes of wound exudate. Commercially known as Mextra©, this layer is particularly effective for moderate-to-severe exudating wounds. It also provides a physical barrier against bacterial infiltration. The primary components of this layer are cellulose (derived from cotton) and lignocellulose (derived from wood).

In Mepilex wound dressings, the Mextra© layer is shielded by a breathable, waterproof film. This film prevents liquid leakage onto clothing or bedding and reduces the risk of contamination. Typically made of polyurethane film, this layer is known as Mepitel© in Mepilex dressings(10). In this research, we aimed to assemble a five-layer wound dressing with a structure similar to that of commercial dressings and compare its performance with the commercially available Mepilex wound dressing. Notably, we incorporated antibacterial properties into our dressing by embedding CS-LL37 nanoparticles (NPs), while utilizing locally sourced materials to minimize costs. This innovative approach not only meets the demand for effective wound care but also highlights resourcefulness and creativity in product development. Figure 1 shows the prepared 5-layer wound dressing.

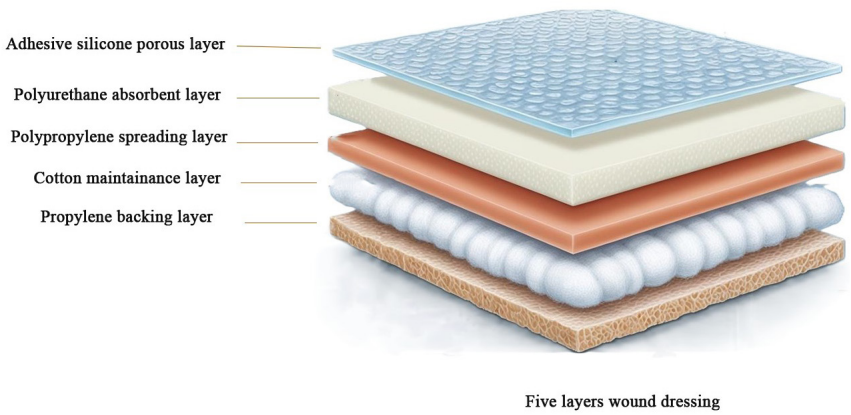

Figure 1. Schematic representation of prepared five layers wound dressing

Materials and Methods

Materials

Sylgard 184 (Cow company, USA), containing the elastomer and curing agent, was prepared. Methylene diphenyl diisocyanate (MDI), PEG6000, polyether polyol, silicon surfactant, tin catalyst, deionized water, and paraffin (all of them from Iran Polymer and Petrochemical Institute) are used for PU synthesis. Chitosan with 95% deacetylation and molecular weight (MW) of 100 to 300 kD (Acros organic company) and LL37 peptide with LLGDFFRKSKEKIGKEFKRIVQRIKDFLRNLVPRTE sequence from Biomatic (Canada) was obtained. Tri poly phosphate (TPP), other solutions, and culture media were obtained from Merck. Hydrophilic polypropylene (100%) and hydrophobic propylene (100%) are prepared by Baftineh and Baftsan company (Malayer, Iran). The cellulosic layer was obtained from Zarin Roya Company (Saveh, Iran).

Methods

Here, the first (silicon) and second (PU) layers were synthesized in the laboratory, while companies prepared other layers.

Synthesis of the silicon layer

The Sylgard 184 silicone elastomer was mixed with its curing agent at a 20:1 ratio. As reported by Mohania *et al.* (2020), adding distilled water (DW) enhances the adhesiveness and porosity of PDMS (1, 11) (supplementary Figure 1). To achieve this, 1 ml of DW was added to 20 ml of the PDMS solution (1). The solution was thoroughly mixed for 10 min, then poured onto a silicon wafer (supplementary Figure 2) and cured at 80 °C for 10 min in an incubator. After curing, a highly adhesive and elastic film formed and was left at room temperature for 24 hr to complete the curing process (11). This resulted in a PDMS layer with moderate adhesiveness and suitable mechanical strength. Finally, holes were created at regular intervals in the layer using a 1 mm punch biopsy tool to facilitate the transfer of wound secretions. The silicone layer after puncture was covered with greaseproof paper to prevent contamination (supplementary information Figure 3-4). For the industrial production of porous PDMS film, we designed the metallic mold, which is represented in the supplementary information (supplementary Figure 5-1). The designed mold contains the negative and positive disks, which match together.

Investigation of cell adhesiveness using the SEM

The prepared silicone layer, the Mepilex silicone layer (Safetec), and a common adhesive tape were compared for their potential to damage the stratum corneum (SC) upon removal. For this evaluation, 1×3-centimeter samples of each material were prepared. The samples were applied to the human skin surface and removed after one minute. The presence of epidermal cells on the surface of each sample was used as an indicator of the extent of SC damage (12).

Investigation of adhesiveness using the tensile machine

Samples of the prepared silicone layer, Safetec layer, and common adhesive tape were cut to 1×2 centimeters and a thickness of 1 mm. Each sample was attached to a 1×3-centimeter section of rat skin, covering 1 centimeter of the skin at both the top and bottom. The remaining 1 centimeter of each sample was clamped into a tensile testing machine (Santam Machine Controller) and stretched from the positive side. The elongation at break was measured for each sample and reported as a relative adhesive strength (13). Figure 2 illustrates the schematic of the tensile test setup.

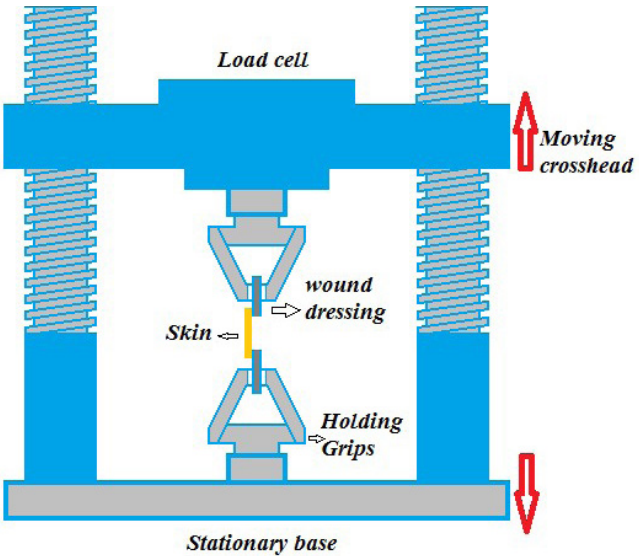

Figure 2. Schematic image of tensile strength measurement device, where two pieces of wound dressing are captured by the skin from above and below and pulled upwards and downwards

Synthesis and characterization of CS-LL37 NPs

Nanoparticle preparation

Bashk*et al.* (2022) synthesized chitosan-LL37 nanoparticles (CS-LL37 NPs), and their method was used in this study. Chitosan (CS) was dissolved in 1% acetic acid to a concentration of 30 mg/ml. A 32 mM solution of the LL37 peptide was added dropwise to the chitosan solution and stirred for 24 hr at 4 °C. Subsequently, a 1 mg/ml solution of tripolyphosphate (TPP) was added over 4 hr at a TPP:CS ratio of 1:3. The nanoparticle solution was then centrifuged for 40 min at 14,000 rpm and 4 °C. The resulting sediment was washed multiple times and freeze-dried for 24 hr (8).

Nanoparticle size and zeta potential

The zeta potential distribution and size of the as-fabricated formulations were measured using dynamic light scattering (DLS) with an SZ-100z Dynamic Light Scattering & Zeta Potential Analyzer (Horiba JobinYvon Co.).

FTIR spectroscopy

In addition, the synthesized chitosan nanoparticles (CS-LL37 NPs) were characterized by Fourier Transform Infrared (FTIR) spectroscopy. The spectra were recorded over the wavenumber range of 500-4000 cm^{-1}.

Encapsulation efficiency (EE) and release profile

The encapsulation efficiency and drug release profile were determined using UV-Visible spectroscopy at the absorption wavelength of LL-37 (215 nm). After centrifuging the CS-LL37NPs, the amount of free LL37 in the supernatant was evaluated using a Shimadzu UV-1208 spectrophotometer. Encapsulation efficiency (EE) was calculated using the following formula:

Encapsulation efficiency (%)=×100

The kinetics of LL37 release from CS-LL37 NPs were evaluated over 1 week. Briefly, CS-LL37NPs were dispersed in phosphate-buffered saline (PBS, 1 mg/ml, pH 7.4) and stirred at 37 °C. At predetermined time points, the samples were centrifuged at 14,000 rpm for 30 min. The supernatant was then separated and replaced with fresh PBS (1 ml). The percentage of LL37 released from the CS-LL37NPs was analyzed using UV-Visible spectroscopy.

Synthesis of PU layer with and without NPs

A mixture was prepared by combining 40 g of polyether polyol, 10 g of PEG6000 (to enhance hydrophilicity and increase the polyurethane's absorption capacity), 1 g of CS-LL37 nanoparticles (NPs), 10 ml of distilled water (DW), 1 g of silicone surfactant, and 2 g of paraffin. The mixture was heated and then cooled to 20 °C. Next, 0.25 g of a tin catalyst was added, and the mixture was stirred for 1 minute. Subsequently, 24 g of methyl diisocyanate (MDI) was incorporated into the mixture, and the mixture was then transferred to a foam mold. The mold was placed in a furnace at 85 °C for 24 hr to complete curing. After curing, the foam was cut into 4 mm sheets (14). For comparison, a control foam without nanoparticles was synthesized using the same method.

Characterization of PU foam with and without CS-LL37 NPs

The properties of the PU foam, including water absorption, water loss, density, and mechanical strength, were investigated. Water absorption and loss were calculated by weighing a specific amount (Wi) of the foam. The foam was immersed in distilled water until fully saturated, then removed and held with tweezers for 10 sec to allow excess water to drain. Any remaining surface water was carefully removed with absorbent paper, and the foam was weighed again (Ww). The samples were then incubated at 37 °C and 50% humidity for 48 hours, after which they were weighed again (Wd). The weight difference (Wd) represents the amount of water lost due to dehydration (15).

The water absorption and weight loss were calculated based on the following relations:

$$\text{Absorption\%}=(Ww-Wi)/Wi *100 \quad \text{Formula 1}$$

$$\text{Weight Loss \%}= (Wi-Wd)/Wi *100 \quad \text{Formula 2}$$

To determine the density, the thickness, length, and width of the samples were measured with a Vernier caliper. The samples were then weighed, and their mass was recorded in grams (g). Density was calculated and expressed in g/cm^3. To evaluate the mechanical properties of PU foam, a 5×2×0.5 cm^3 sample was subjected to tensile testing. The force at elongation at break was measured to assess mechanical strength, elongation capacity, and Young's modulus (15). The tensile tests were conducted at a rate of 10 mm/min and repeated three times for accuracy.

Attachment of 5 layers together

Layer assembly was performed under a laminar flow hood. The silicone layer was covered with wax paper to prevent contamination before subsequent layers were added. To assemble the five layers, the first silicone layer was attached to the fifth propylene layer, with the remaining three layers enclosed between them. During this process, the silicone layer was partially cured before the subsequent layers were attached. This allowed the three inner layers, which have smaller dimensions (8 cm), to be securely enclosed by the first and fifth layers, both of which measure 10 cm. Once assembled, sufficient time was allowed to ensure the complete curing of the silicone layer.

Antibacterial assay

To evaluate the antibacterial effectiveness of the prepared wound dressing, the first two layers—silicone and polyurethane (SiPU)—which come into direct contact with the wound (with and without CS-LL37 NPs), were compared with Mepilex. The antibacterial activity of each sample was assessed by measuring the zone of inhibition (ZOI) against *Staphylococcus aureus* (ATCC 25923)(16). Nutrient agar medium was used for bacterial growth. Circular sections of each wound dressing, measuring 0.5 cm in diameter, were placed on the medium and incubated at 37 °C for 24 hours. An Azithromycin (AZM) antibiotic disk was used as a positive control.

Cell toxicity assay

The cytotoxicity of the prepared wound dressing was evaluated on human skin fibroblast cells (HNFF-P18) using the MTT assay. The samples were divided into three groups: the commercial Mepilex layer, and a two-layer dressing (silicone in direct contact with the skin, plus a PU layer, designated SiPU), prepared either with or without CS-LL37 NPs. The skin fibroblast cells were cultured in DMEM medium supplemented with 10% fetal bovine serum (FBS) and incubated at 37 °C in a 5% CO_2 incubator. After 24 hr of incubation in 24-well plates, the cell density reached 1×10^4 cells per well in 500 µl of medium. After cell seeding, small parts of each sample were placed in wells. The plates were then incubated for 24, 48, and 72 hr. Following incubation, the plates were washed, and 100 µl of MTT solution (0.5 mg/ml in PBS) was added to each well. The plates were further incubated at 37 °C for 30 min to allow the formation of purple formazan crystals resulting from MTT reduction. The experiment was repeated three times, and absorbance was measured at 570 nm using an ELISA reader (17).

Animal test

Sixteen female Wistar rats (approved by the Experimental Animal Welfare and Ethics Committee at Baqiyatallah Medical University under Certificate No. IR.BMSU.BLC.1402.027) were used for the study. The rats were 7 weeks old and weighed between 220 and 240 Grams. They were anesthetized via intraperitoneal injection of a ketamine-xylazine mixture (9:1 ratio), and a 20 mm diameter wound was created on the dorsal area using a punch biopsy tool(18). The rats were divided into four groups:

1. A negative control group (untreated),
2. A group treated with the commercial Mepilex wound dressing,
3. A group treated with the 5-layer wound dressing containing CS-LL37 NPs, and
4. A group treated with the 5-layer wound dressing without NPs.

Wound closure was monitored by measuring wound diameter with ImageJ on days 4, 7, 10, and 14 post-wounding. The remaining wound area was calculated using Formula 1 and expressed as a percentage of wound closure.

Wound closure percentage=×100

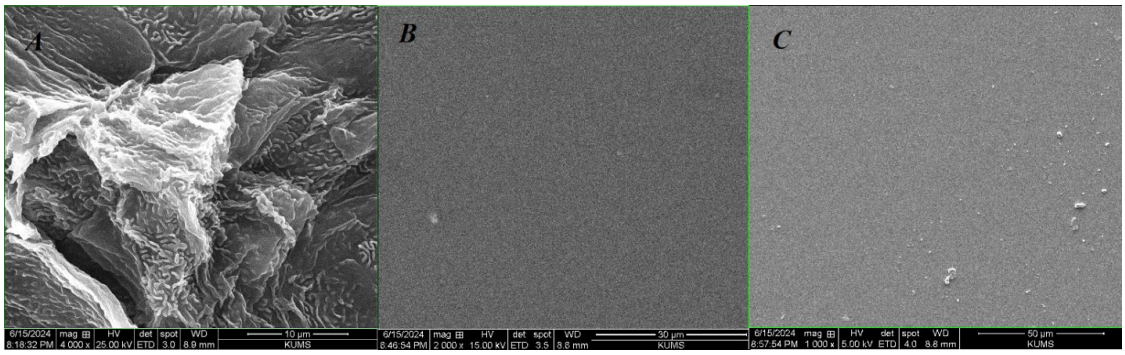

Figure 3. The SEM image of common tape (A), commercial Mepilex Border wound dressing (B), and our silicone wound dressing (C) after attachment and separation from the skin

Histology of healed wounds

On the 15th day of wound healing, the rats were euthanized using an overdose of ketamine-xylazine. The healed wound area was excised for histological analysis and preserved in formalin buffer. Tissue samples were sectioned using a microtome and stained with hematoxylin and eosin (H&E). The stained slides were examined under a digital light microscope (Olympus, Japan) to evaluate tissue remodeling indicators(18).

Statistical analysis

Here, the experiments were performed in triplicate and expressed as the mean ± standard deviation. The method of analysis was ANOVA (one-way (Dunnett's t-test) in SPSS version 27.0. and GraphPad Prism version 9.

Results

Cell attachment investigation using the SEM

This is a significant finding, as it highlights the difference in cell attachment between conventional wound tape and silicone-based dressings, such as Mepilex and the silicone wound dressing developed in this study. Figure 3A illustrates how common wound tape removes a large number of epidermal cells from the skin surface. In contrast, the silicone dressings (Figure 3B and 3C) demonstrate minimal separation of epidermal cells, indicating their suitability for use on vulnerable or fragile skin. The presence of epidermal cells on the surfaces of both Mepilex and our silicone wound dressing further confirms that these products are less likely to cause damage or trauma during application or removal. This underscores the advantage of moderate adhesion, as provided by silicone dressings, in preserving skin integrity and fostering an optimal wound-healing environment. The more SEM Figures show details about what happens to the skin cells after separation of every wound dressing (supplementary Figure12-17).

Determination of skin attachment force using the tensile machine

In this study, a test was conducted to compare the adhesion force of two wound-dressing materials. Evaluating adhesion force using a tensile machine is a critical step in assessing the performance and effectiveness of wound dressings. By comparing the adhesion forces of various samples, it is possible to determine which material offers better retention and security when applied to the skin. Figure 4 illustrates the force curve at the point of separation, providing insight into the materials' adhesive properties.

According to Figure 4, the adhesion force for standard tape is 17.6 N, which causes skin damage and separates the epidermal layer upon removal. In contrast, Mepilex Border, a standard wound dressing for EB patients, exhibits an adhesion force of 3.45 N, making it suitable for skin application without causing harm during removal. Our 5-layer wound dressing, with an adhesion force of 3.2 N, exhibits a force similar to Mepilex, suggesting it is also safe for sensitive skin, such as that of EB patients.

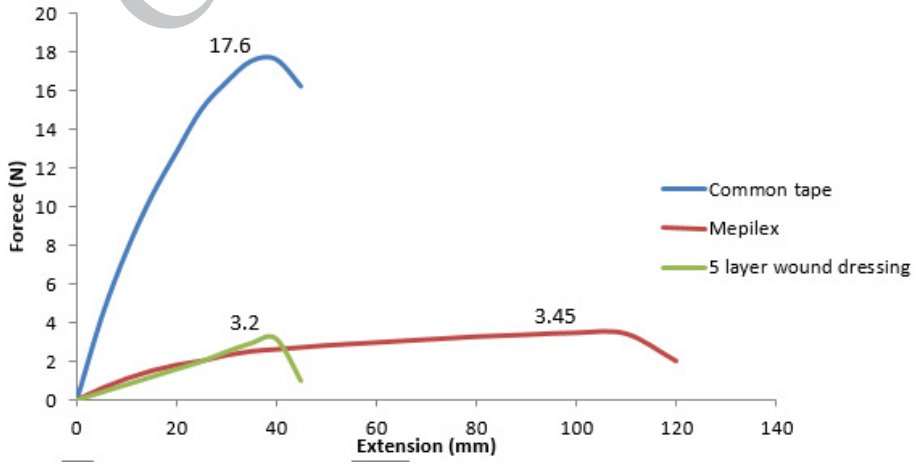

Figure 4. The force curve (N) versus extension (mm) for measuring sample adhesion

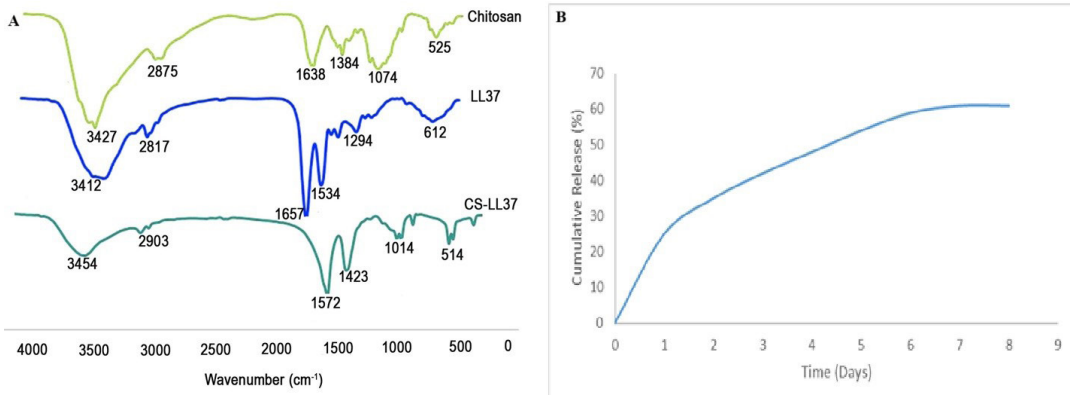

Figure 5. The FTIR (A) and release kinetic of LL37 from the CS NPs (B)
FTR: Fourier transform infrared; NPs: Nanoparticles; CS: Chitosan

Characterization of CS-LL37 NPs

The FTIR spectroscopy confirmed the successful loading of the LL37 peptide into the chitosan NPs (Figure 5A). The FTIR spectrum of chitosan shows O-H/N-H stretching vibrations at 3427 cm^{-1}, C-H stretching at 2875 cm^{-1}, Amide I (C=O) at 1638 cm^{-1}, and C-O-C stretching at 1074 cm^{-1}.FTIR Spectrum of LL37 peptides shows characteristic amide bands at 1657 cm^{-1} (Amide I, C=O stretching), 1534 cm^{-1} (Amide II, N-H bending/C-N stretching), and 1294 cm^{-1} (Amide III, C-N/N-H vibrations). A broad peak at 3412 cm^{-1} corresponds to O-H/N-H stretching, while the 2817 cm^{-1} peak represents C-H stretching in amino acid side chains. The FTIR spectrum of CS-LL37 NPs shows key interactions: the amine peak shifted from 1638 to 1572 cm^{-1}, confirming LL37 binding to chitosan's amino groups. The reduced intensity at 1074 cm^{-1} indicates altered glycosidic bonds, while the disappearance of LL37's 1657 cm^{-1} peak demonstrates physical chitosan-peptide interactions. These changes collectively verify successful nanoparticle formation.

SEM images (Figure 6) revealed sizes of ~90 nm for CS-LL37 NPs and ~60 nm for CS NPs. The zeta potential values were +16 for CS-LL37 NPs and +18 for CS NPs. The encapsulation efficiency (EE) and drug loading capacity were 87.9% and 10.17%, respectively. The release kinetics of LL37 from the CS NPs demonstrated sustained release over 6 days (Figure 5B), indicating enhanced efficacy. The DLS results show larger values due to the hydrodynamic diameter, as presented in Table 1.

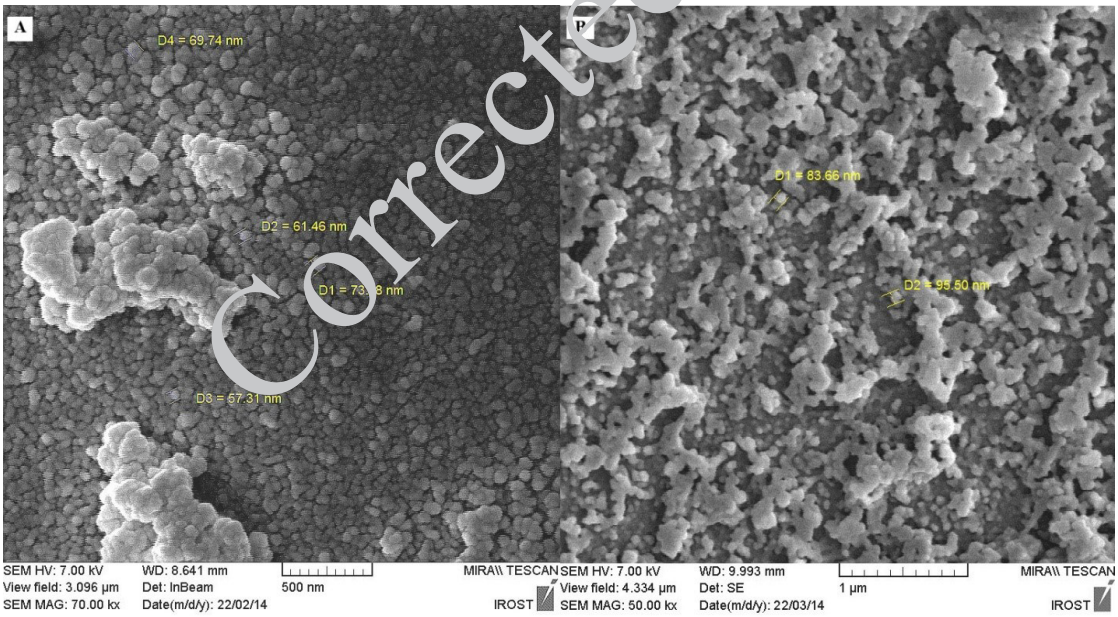

Figure 6. The SEM image and CS NPs (A) and CS-LL37 NPs (B)
NPs: Nanoparticles; CS: Chitosan

Table 1. Actual size of NPs measured by SEM, the hydrodynamic size by DLS, zeta potential, and polydispersity index (PDI)

Nanoparticle	SEM Size	Hydrodynamic diameter by DLS	Zeta potential	PDI
CS NPs	60	203	+18	0.257
CS-LL37 NPs	90	319	+16	0.311

NPs: Nanoparticles; DLS: Dynamic light scattering

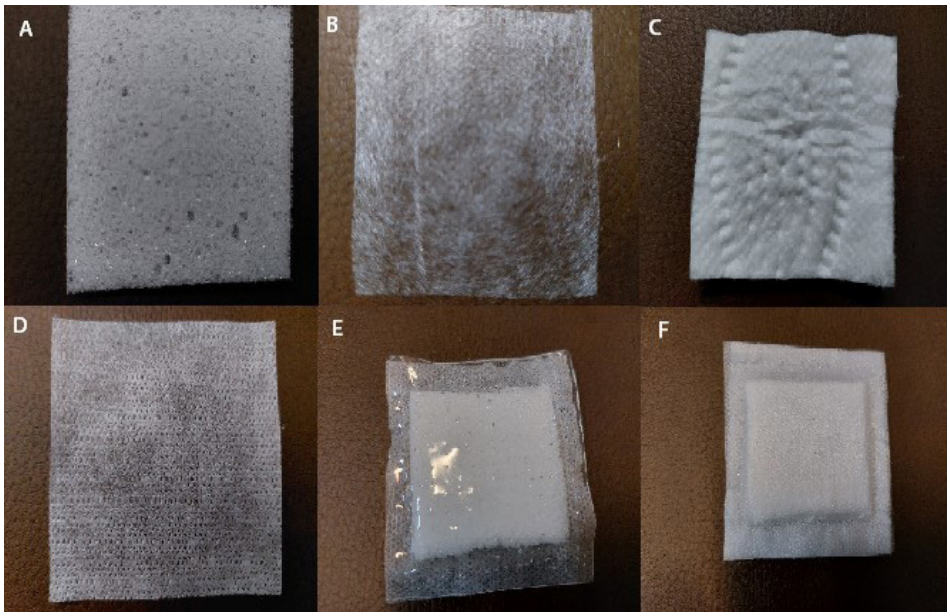

Figure 7. The cut-off PU foam (A), the spreading layer from polypropylene (B), the maintaining layer from commercial pulping fluff (C), the hydrophobic backing layer from propylene (D), the assembled five layers from front view (E), and the backing view (F)
PU: Polyurethane

PU foam production with and without CS-LL37 NPs

The bulk PU foam, prepared as described in sections 2–3, was cut into 2–3-mm-thick sheets using an industrial fabric cutter. These sheets can be further shaped as needed using scissors. To ensure potential disinfection, the PU sheets can be exposed to UV light. Figure 7A illustrates the prepared foam after cutting.

Physical and mechanical characteristics of PU foam

In Table 2, the water absorption, weight loss, density, and Young's Modulus of PU foam are listed.

Maintaining an optimal moisture balance in wound care is essential for promoting effective healing. The information provided underscores the importance of managing excessive exudate while preventing the wound from drying out. Wound dressing materials with high swelling ratios, such as polyurethane foams, are particularly beneficial for absorbing excess exudate and maintaining a moist environment. In addition to fostering an environment conducive to growth factors and cell regeneration, these dressings help prevent tissue damage from excessive moisture or dryness. By effectively controlling exudate levels and maintaining proper moisture balance, PU foam and similar materials can significantly enhance the healing process, especially in chronic wounds (19).

As shown in Table 2, the inclusion of CS-LL37 NPs in PU foam has a minimal effect, which can be attributed to the functional groups of chitosan. However, combining PU foam with a maintenance cellulose layer significantly increases water absorption, doubling the material's capacity. This highlights the maintenance layer's exceptional ability to absorb liquids, facilitated by its smaller pores, which effectively retain liquid within the layer.

Preparation of the third, fourth, and fifth layers of wound dressing

These three layers are sourced from the diaper and sanitary napkin industries. The spreading layer, which has hydrophilic properties, is made of nonwoven polypropylene (Figure 7B). The cellulose layer is composed of cotton linter (Figure 7C), and the hydrophobic backing layer is made of polypropylene (Figure 7D), as illustrated in Figure 7.

The 5-layer attachment

The five-layer assembly was achieved by attaching the first and fifth layers. When the silicone layer is in a semi-cured state, the other layers and the fifth layer are adhered to it, and continuous curing ensures a stable attachment. Figure 7E and 7F show the complete wound dressing from the top and bottom views, respectively.

The antibacterial assay

In Figure 8, the antibacterial activity of each sample was evaluated against S. aureus, a major skin pathogen. In each plate, an Azithromycin disc was placed at the center, creating an inhibition zone. The cut Mepilex disc (Figure 8A) and the sample prepared from a two-layer wound dressing (silicone adhesive and PU foam) (Figure 8B)

Table 2. Physical and mechanical properties of PU foam with or without NPs, along with the spreading and maintaining layer

Properties	Water absorption (%)	Water loss (%)	Density (g/cm^3)	Young modulus (MPa)
PU foam	95.6	0.05	41.1	0.036
CS-LL37 NPs containing PU foam	98.4	0.06	41.3	0.038
PU foam with a spreading and maintenance layer	185	0.01	13.8	0.032

NPs: Nanoparticles; PU: Polyurethane

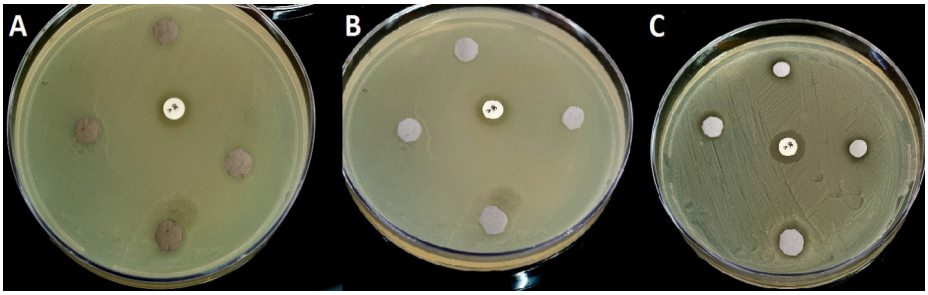

Figure 8. The microbial growth inhibition test
The antibiogram Azitromycine disk is present as a control sample in the center of every plate. The commercial Mepilex without microbial growth inhibition (A), the two-layer of our wound dressing mean SiPU without NPs (B), and the two-layer of SiPU with CS-LL37 NPs (C) were shown.
NPs: Nanoparticles; PU: Polyurethane; CS: Chitosan

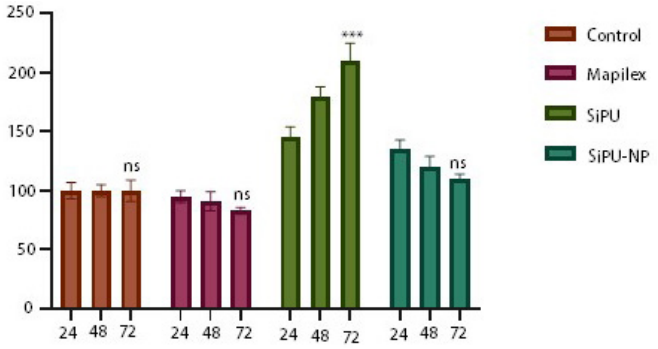

Figure 9. Skin fibroblast cell growth curve with wound dressing samples
Values are means±SD (n=72) one-way ANOVA followed by Tukey's multiple comparisons test. $P \leq 0.05$. Data compared with control.

did not exhibit any inhibition zone. However, the sample prepared from the silicone layer with PU foam containing CS-LL37 nanoparticles (NPs) showed a narrow inhibition zone (Figure 8C).

Cell culture assay

The biocompatibility of the wound dressings was evaluated using the MTT assay. Cell viability in a 24-well plate was measured at 24, 48, and 72 h after incubation at 37 °C. As shown in Figure 9, none of the three wound dressing samples exhibited toxicity toward fibroblast skin cells. In some cases, an increase in cell count was observed. This cell proliferation is primarily attributed to the scaffold-like properties of the wound dressing.

The in vivo test

In this study, we compared a 5-layer wound dressing with and without CS-LL37 NPs with Mepilex Border. The rate of wound closure was calculated on the 4th, 7th, 10th, and 14th days using ImageJ software. Figure 10 clearly illustrates the wound healing process. By the 14th day, all treatment groups showed similar results, with over 80% wound closure observed in rats treated with each wound dressing type. Table 3 provides detailed data on the extent of wound closure from days 4 to 14.

Histology of healed wounds

In Figure 11, the histology of healed wounds shows remodeling, evidenced by hair follicles, sebaceous glands, fatty glands, keratinized tissue, blood vessels, and white adipose tissue. Notably, the samples treated with the 5-layer wound dressing containing CS-LL37 NPs exhibit

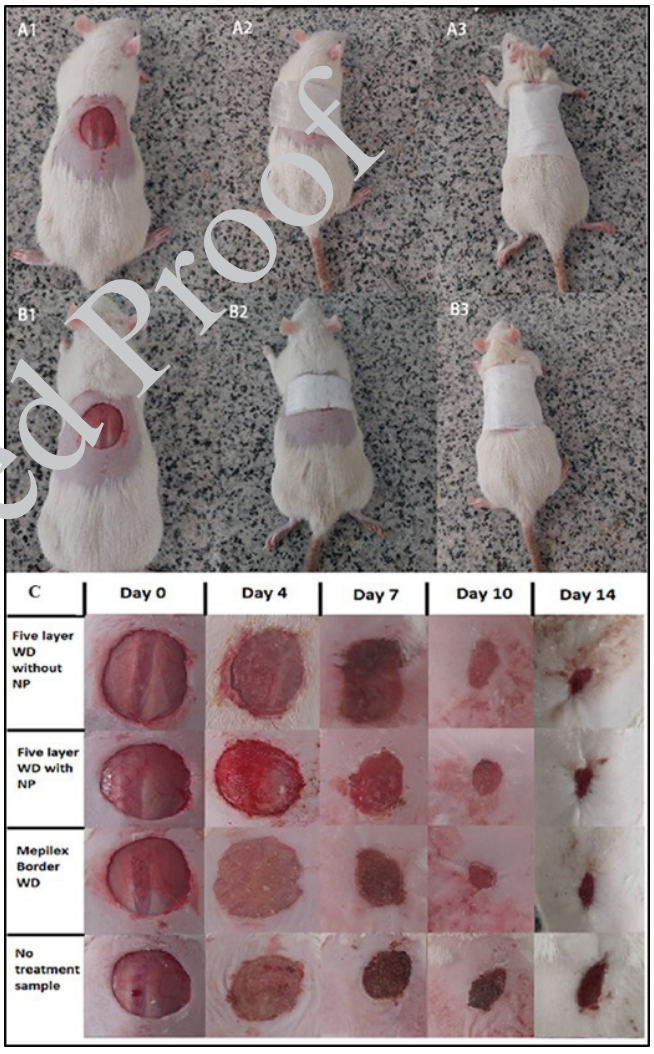

Figure 10. The *in vivo* analysis of wound healing on female Wistar rats
The A1, A2, and A3 show wound creation, using 5-layer wound dressing and stabilizing by surgical tape, respectively. The B1, B2, and B3 show this period in Mepilex wound dressing usage.

faster remodeling, with larger hair follicles and accelerated development of sebaceous and fatty glands. In contrast, the untreated samples show fewer signs of remodeling than the treated groups and exhibit a greater presence of collagen tissue.

In the histology of wounds treated with the anti-adhesive electrospun PDMS-PU wound dressing, signs of effective wound healing were observed, including an

Table 3. Percentage of wound closure on different days

	Day 4	Day 7	Day 10	Day 14
Five-layer without NPs	11%	29%	71%	83%
Five-layer with CS-LL37 NPs	15%	60%	75%	84%
Mepilex Border	8%	58%	76%	85%
Control	12%	55%	64%	72%

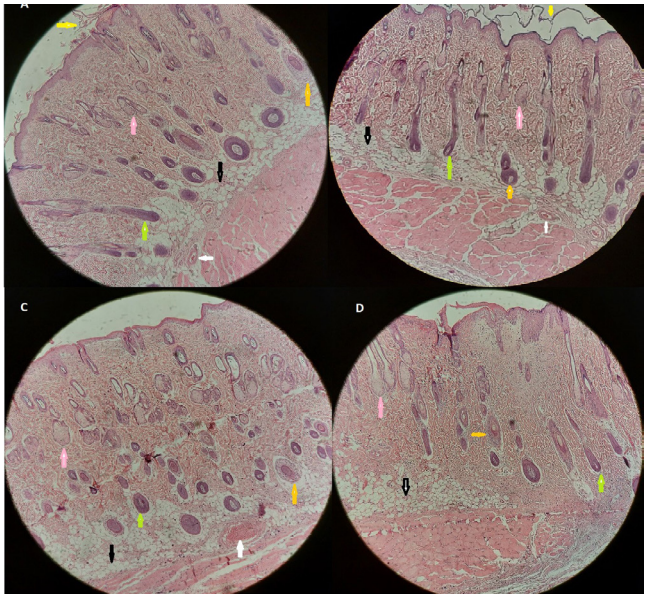

Figure 11. Microscopic images at magnifications of 100X from the histology of treated wounds of rats on the 15th day
The histology of wounds treated by out 5-layer wound dressing without the NPs (A), the treated wound with 5-layer wound dressing containing the CS-LL37 NPs (B), the treated wound with Mepilex Border (C), and untreated (D) wounds. The arrows show sebaceous glands (orange), hair follicles (green), fatty glands (pink), blood capillaries (white), white adipose tissue (black) and keratination tissue (yellow).
NPs: Nanoparticles; CS: Chitosan

intact epidermis, absence of inflammation and necrosis, complete vascularization, and the formation of connective tissue. The deposition of mature collagen in samples treated with PDMS-PU nanofibers indicates the lowest level of skin damage, highlighting the dressing's effectiveness in promoting healing(4).

Discussion

An ideal adhesive should securely keep the dressing in place for the appropriate duration, minimizing the risk of skin maceration around the wound. It must also allow safe removal of the dressing without damaging the wound or surrounding skin. Additionally, it should be non-irritating, non-sensitizing, and leave no residue on the skin. The adhesive should provide the right balance of tackiness for both immediate and long-term adhesion, while still allowing adjustments to the dressing without compromising the dressing's stability. The optimal duration for wearing the dressing depends on factors such as exudate levels, signs of infection, manufacturer recommendations, and the overall condition of the wound. Typically, this duration should not exceed 7 days and should be tailored to the patient's specific needs and the wound (20).

Clinical trials have been conducted across various wound types to compare Mepitel with traditional wound care options, including paraffin gauze, absorbent pads, and bandages. These trials are valuable for identifying which dressing offers superior outcomes in healing rates, patient comfort, and ease of application and removal. The adhesive properties of wound dressings play a critical role in patient comfort and the overall effectiveness of treatment. By including a diverse range of wounds in these trials—such as skin grafts, burns, chronic wounds like diabetic ulcers, and congenital skin disorders like EB and mycosis fungoides—researchers gain important insights into the versatility and applicability of the evaluated products(21).

EB is a genetic condition characterized by extremely fragile skin that blisters, erodes, and scars from minor friction or trauma. Selecting appropriate dressings is crucial for managing EB, as traditional options like paraffin gauze can adhere to the skin and cause further damage during removal due to the skin's fragility. Mepitel has demonstrated success in treating EB because it adheres gently to intact, dry peri-wound skin without sticking to the moist wound bed, enabling painless, trauma-free removal. It has been effectively used to treat EB patients, reducing pain and anxiety during dressing changes. Mepitel conforms well to body contours, and its porous structure allows exudate to pass through into an absorbent secondary dressing. Additionally, it is permeable to topical antibacterial agents, aiding in the management of secondary infections. This dressing can remain in place for 3–4 days, maintaining a moist wound environment, promoting healing, and minimizing damage, with epithelialization often occurring within a month(22). The prepared silicone layer, with its mild adhesive properties, porous structure, and flexibility, mimics the characteristics of Mepitel. The foam, diffusion, and maintenance layers effectively absorb exudate, eliminating the need for secondary dressings to manage wound secretions. Furthermore, incorporating CS-LL37 NPs enhances the wound dressing by enabling the use of external topical antibacterial agents, thereby improving its overall functionality.

The adhesion force of PDMS was measured using an indentation method. This setup involves applying a controlled load to a soft sample using a hard, spherical Atomic Force Microscopy (AFM) probe while measuring the interaction force and probe displacement. During the approach phase, when the probe moves toward the sample, the interaction force remains constant (zero). As the probe indents the sample, circular deformation occurs in the contact area, increasing with the applied load. The force-indentation curves obtained during this process provide valuable insights into the sample's mechanical properties. Additionally, this setup allows for the assessment of adhesion. During retraction, the probe does not detach from the surface until the pull-off force exceeds the adhesion forces. This pull-off force serves as a measure of the adhesion strength between materials (23).

The previously described method for measuring PDMS adhesion force is prone to high error and requires extensive calculations to determine the force accurately. In contrast, our approach utilizes a qualitative-quantitative method, using Safetec adhesiveness as a benchmark for wound dressing evaluation. This method is more advantageous due to its cost-effectiveness, accessibility, simplicity (eliminating the need for a circular probe), and reduced computational complexity.

Encapsulating peptides in nanoparticles (NPs) offers the

significant advantage of extending their shelf life. Peptides generally have a very short shelf life due to enzymatic degradation, often lasting only a few hours. To address this, encapsulating peptidic drugs within NPs is highly recommended. For instance, loading the LL37 peptide into chitosan NPs can increase its shelf life to several days, enhancing its stability and usability. Prolonged release of antibacterial materials can significantly reduce the risk of bacterial invasion into the wound, thereby decreasing the frequency of dressing changes. This not only enhances patient comfort but also improves overall wound management(24). Additionally, the antibacterial properties of chitosan can enhance LL37 efficacy through a synergistic effect. This highlights the fascinating potential of chitosan nanoparticles in combination with the LL37 peptide. The enhanced antibacterial activity and superior biofilm-reducing capability of CS-LL37 nanoparticles against methicillin-resistant *S. aureus* (MRSA), compared with chitosan or LL37 alone, represent significant findings (8). The combination of chitosan with polyurethane in drug-carrying structures has demonstrated promising results. The formation of hydrogen bonds between chitosan and polyurethane molecules facilitates the uniform dispersion of chitosan within the polyurethane matrix, thereby improving mechanical properties, tensile strength, flexibility, and elastomeric behavior. Additionally, the reaction between the urethane group in polyurethane and the NH2 group in chitosan forms strong intermolecular hydrogen bonds without steric hindrance. This interaction enables versatile applications of chitosan in polyurethane structures, such as serving as a chain extender or cross-linking agent. Moreover, modified forms of chitosan have been shown to enhance the mechanical properties, thermal stability, biodegradability and antibacterial activity of polyurethane. These findings underscore the potential of chitosan-polyurethane composites for a wide range of biomedical applications, thanks to their superior properties (25).

The narrow inhibition zone observed in the PU foam containing NPs indicates a slight release of LL37 from the chitosan NPs. The medium's humidity drives the release of the LL37 peptide, which subsequently inhibits bacteria. This highlights the superiority of LL37-NPs over antibiotics and metallic NPs in several aspects. The rise of antibiotic resistance due to excessive antibiotic use and the toxicity of metal particles underscores the need for biological alternatives such as the LL37 peptide. The LL37 peptide's ability to resist proteolytic digestion through membrane attachment enables it to effectively kill bacteria. Additionally, membrane attachment induces changes in bacterial morphology and leads to complete lysis (26). The innate immune system acts as the body's first line of defense against pathogens. Skin keratinocytes form a multilayered epidermis, creating a protective barrier between the internal body and the external environment. When the epidermis is compromised due to injury, pathogens can easily invade. Bacterial contact, inflammation, and injury trigger keratinocytes to produce the human cathelicidin antimicrobial peptide 18 (hCAP18/LL37). Granulocytes and mast cells also contribute to LL37 production. When LL37 is highly expressed in the wound area, it promotes keratinocyte migration to the wound site through a positive feedback mechanism. Additionally, LL37 influences endothelial and inflammatory cells, such as neutrophils, monocytes, and T cells, attracting them to the wound site to aid in healing (27). Prolonged application of wound dressings requires extended disinfection capabilities. Encapsulating the antibacterial peptide LL37 in chitosan NPs enables sustained release over 6 days, a key advantage of this approach. The antibacterial efficacy of LL37 is further enhanced by chitosan, a natural antibacterial agent known for its antibiofilm properties and synergistic effects with other antimicrobial agents (8).

The adhesive properties of PDMS facilitate cell attachment in culture media and promote cell division. As a versatile material in tissue engineering, medical engineering, and microfluidics, PDMS has demonstrated excellent biocompatibility in cellular and tissue culture environments. It is an effective material for both micro- and macro-scale cell culture. The affordability, elasticity, gas permeability, and transparency of PDMS make it an ideal choice for cellular and tissue applications. Enhancing the surface properties of PDMS to improve adhesion can further promote cell growth in culture media (28). The enhancement of fibroblast cell growth in the presence of CS-LL37 nanoparticles incorporated into PCL/PVA nanofibers has been confirmed (29). However, the nanofiber structure only has a higher effect on cell growth (30), but the data indicate that CS-LL37 NP has no toxic effect on cells and that the reduction in cell number has not occurred (29). The free LL37 peptide has been shown to reduce cell growth due to its anti-fibrotic properties, which decrease fibrotic tissue formation in the wound area. The gradual release of LL37 from chitosan NPs over 72 hr has been associated with the peptide's inhibitory effect on cell viability. This anti-fibrotic mechanism is attributed to LL37's ability to downregulate the gene expression of collagen I and III (31).

The PU foam acts as a scaffold for cell growth. Studies have demonstrated that human fibroblast cells experience a 10-fold increase in population between 4 and 30 days of incubation. This highlights the significant role of the foam in promoting cell proliferation and supporting wound treatment (32). It was evident that the Mepilex wound dressing had no significant effect on cell growth and proliferation. Although the exact composition of this dressing is not fully disclosed, research involving the culture of primary keratinocytes in the presence of Mepilex showed a reduction in cell numbers over time, indicating a slower rate of cell division. Additionally, the cultured cells exhibited increased apoptosis and morphological changes (33).

The use of PDMS in wound dressing production is relatively limited. However, its excellent characteristics—such as biocompatibility, breathability, flexibility, and chemical stability—make it a highly suitable candidate for wound-dressing applications (2). The two primary factors contributing to delayed wound healing are infection and wound-dressing adhesion. Early detection of pathogenic infections and minimizing dressing-to-wound attachment are critical. To address these challenges, anti-adhesion wound dressings made from co-spun PLGA and PDMS have been developed. These dressings prevent secondary damage to the wound during dressing changes and accelerate the healing process. Furthermore, incorporating antibacterial peptides helps prevent infections and enhance the overall quality of healing (34). Furthermore, co-spun PDMS and PU synthesis yields an anti-adhesive, biocompatible wound dressing that demonstrates excellent wound-healing performance *in vivo*. This makes it a highly suitable candidate for the production of anti-adhesion, breathable wound dressings (4). The *in vivo* wound-healing effects of three types of silicone wound

dressings, compared with a control, are linked to their anti-adhesion and breathability. These characteristics, combined with the inclusion of antibacterial NPs, accelerate the healing process and prevent infections. Additionally, the anti-fibrotic effect of LL37 helps prevent scar formation.

In recent research, Chen *et al.* (2024) fabricated a multilayered bandage with reversible adhesive properties. The bandage features a covalently crosslinked poly (acrylamide) (PAAm) hydrogel as the intermediate layer, which provides moisture and supports cell growth in the wound area. The dynamically covalently bonded poly(vinyl alcohol)/boric acid (PVA/BA) layer enhances the dressing's flexibility and durability. The outer layer, composed of covalently crosslinked PDMS, acts as a barrier against external contaminants while allowing gas exchange. This environmentally stable, biocompatible, and reversibly adhesive multilayered bandage represents a significant advancement in wound care. However, a potential issue is the dissolution of the PVA/BA adhesive film under continuous water exposure, which could limit its practical application. Achieving wound closure in just 2 days in a murine wound healing model is an impressive result. Given these advantages, further exploration of this dressing's performance in clinical settings and comparisons with existing products would be valuable. While exposure to body moisture and environmental humidity is inevitable, our 5-layer dressing maintains adhesion even in humid conditions and during bathing. These features make it highly suitable for long-term use and daily activities, enhancing its practicality for patients (35).

The development of a silicone bioadhesive dressing by Huang *et al.* (2024) featuring a shear stiffening adhesive (SSA) represents a significant advancement in wound care technology. The incorporation of poly(vinylpyrrolidone)-iodine (PVP-I) as an antibacterial agent further enhances its potential for effective wound management. The dressing's controlled adhesion response—allowing easy removal during deliberate, slow actions while maintaining high strength under rapid force—demonstrates its practicality for clinical use. However, the continuous release of free iodine from the silicone bioadhesive dressing with SSA into the surrounding environment raises concerns, as it may contribute to inflammation and other adverse effects. While the increased presence of hair follicles and subcutaneous glands in histology indicates positive healing effects attributed to the silicone dressing, careful regulation of the PVP-I dose and its release rate is essential. Failure to control these factors could lead to increased tissue inflammation, potentially hindering recovery. In contrast, the use of natural antibacterial substances such as LL37 and chitosan in wound dressings offers advantages, including reduced environmental impact and a lower risk of inflammation, compared to synthetic agents like PVP-I. These natural substances typically require less stringent dose regulation, as they are less likely to cause toxicity or adverse reactions when released into the environment. The ability of a wound dressing to maintain consistent adhesion and prevent skin damage during removal is a critical factor in patient care. The fact that our dressing offers this advantage over alternatives, such as SSA dressings, is a significant benefit and a strong selling point (36).

Conclusion

This research aimed to develop a 5-layer wound dressing capable of treating sensitive skin conditions, such as those in EB patients, and managing exudate. Our goal was to create a wound dressing that outperforms commercial, expensive alternatives. A key feature of this dressing for sensitive EB patient skin is its moderate adhesion, as confirmed by two tests. The first test demonstrated the absence of epidermal cell separation, as verified by SEM imaging, and the second test measured the adhesion force using a tensile machine. The adhesion force of Mepilex was 3.45 N, while our 5-layer wound dressing was 3.2 N, indicating comparable performance. The successful physicochemical properties and *in vivo* wound healing results, relative to Mepilex, suggest that this new wound dressing offers enhanced therapeutic capabilities at a reduced cost.

Acknowledgment

The authors would like to thank the Clinical Research Development Unit of Baqiyatallah Hospital for all their support and guidance during carrying out this study. We want to thank the guidance and support provided by the Research and Technology Comprehensive Laboratory (RTCL) of Baqiyatallah University of Medical Sciences.

Fundind

This research received no external funding.

Ethics Statement

The research experiments detailed in this article were approved by the research ethics committee of Baqiyatallah University ([2023] IACUC Number: IR.BMSU.BLC.1402.027).

Authors' Contributions

M R was responsible for conceptualization, formal analysis, investigation, and writing the original draft. M MM handled data curation, investigation, and also contributed to the original draft. RA T and H D contributed to conceptualization, supervision, securing funding, and reviewing and editing the manuscript.

Conflicts of Interest

The authors have no conflicts of interest.

Declaration

The ChatGPT tool was used for the design of the graphical abstract. The authors also used AI-assisted technologies (Grammarly and iThenticate) to rephrase, reduce plagiarism, and improve language and grammar. After using these tools/services, the authors reviewed and edited the content as needed and take full responsibility for the publication's content.

References

1. Mohania V, Deshpande TD, Singh YR, Patil S, Mangal R, Sharma A. Fabrication and characterization of porous poly (dimethylsiloxane)(PDMS) adhesives. ACS Applied Polymer Materials 2020;3:130–140.
2. Du W, Zhang Z, Fan W, Gao W, Su H, Li Z. Fabrication and evaluation of polydimethylsiloxane modified gelatin/silicone rubber asymmetric bilayer membrane with porous structure. Materials & Design 2018;158:28–38.
3. Menon A, Sreeram P, Vinod A, Naiker V, Nandana M, David DA, *et al.* Polyurethane (PU): Structure, properties, and applications.

Handbook of Thermosetting Foams, Aerogels, and Hydrogels: Elsevier; 2024. p. 67–92.
4. Yu Y, Xu G, Zhao P, Zhang J. Biocompatible, robust, waterproof and breathable PDMS-based PU fibrous membranes for potential application in wound dressing. Mater Today Commun 2024;38:107870.
5. Dos Santos MR, Alcaraz-Espinoza JJ, da Costa MM, de Oliveira HP. Usnic acid-loaded polyaniline/polyurethane foam wound dressing: preparation and bactericidal activity. Mater Sci Eng C 2018;89:33–40.
6. Usman A, Zia KM, Zuber M, Tabasum S, Rehman S, Zia F. Chitin and chitosan based polyurethanes: A review of recent advances and prospective biomedical applications. Int J Biol Macromol 2016;86:630–465.
7. Ramos R, Silva JP, Rodrigues AC, Costa R, Guardão L, Schmitt F, *et al*. Wound healing activity of the human antimicrobial peptide LL37. Peptides 2011;32:1469–1476.
8. Rashki S, Safardoust-Hojaghan H, Mirzaei H, Abdulsahib WK, Mahdi MA, Salavati-Niasari M, *et al*. Delivery LL37 by chitosan nanoparticles for enhanced antibacterial and antibiofilm efficacy. Carbohydr Polym 2022;291:119634.
9. Lee SM, Park IK, Kim YS, Kim HJ, Moon H, Mueller S, *et al*. Physical, morphological, and wound healing properties of a polyurethane foam-film dressing. Biomater Res 2016;20:15.
10. Barrett S. Mepilex®> Ag: An antimicrobial, absorbent foam dressing with Safetac®> technology. Br J Nurs 2009;18:S28–S36.
11. Sales FC, Ariati RM, Noronha VT, Ribeiro JE. Mechanical characterization of PDMS with different mixing ratios. Procedia Struct Integr 2022;37:383–388.
12. White R. Evidence for atraumatic soft silicone wound dressing use. Wounds UK 2005;1:104–109.
13. Nussinovitch A, Gal A, Padula C, Santi P. Physical characterization of a new skin bioadhesive film. Aaps Pharmscitech 2008;9:458–463.
14. Yildirim A, Yilgor E, Yilgor I. Polyurethane synthesis revisited: Effect of solvent, stoichiometry, and temperature on the reaction of MDI with polyether glycols. Polymer 2025;326:128340.
15. Namviriyachote N, Lipipun V, Akkhawattanangkul Y, Charoonrut P, Ritthidej GC. Development of polyurethane foam dressing containing silver and asiaticoside for healing of dermal wound. Asian J Pharm Sci 2019;14:63–77.
16. Bužarovska A, Dinescu S, Lazar AD, Serban M, Pandele-Cusu J, Gabioru GG, Costache M, *et al*. Nanocomposite foams based on flexible biobased thermoplastic polyurethane and ZnO nanoparticles as potential wound dressing materials. Mater Sci Eng C 2019;104:109893.
17. van Kooten TG, Whitesides JF, von Recum AF. Influence of silicone (PDMS) surface texture on human skin fibroblast proliferation as determined by cell cycle analysis. J Biomed Mater Res 1998;43:1–14.
18. Samavati SS, Kashanian S, Derakhshankhah H, Rabiei M, Sajadimajd S, Fakhri S, *et al*. Accelerated wound healing through tannin-rich Jaft extract, concentration-dependent efficacy and mechanistic insights from Quercus brantii ointment formulations. Sci Rep 2025;15:29004.
19. Morena AG, Stefanov I, Ivanova K, Pérez-Rafael S, Sánchez-Soto M, Tzanov T. Antibacterial polyurethane foams with incorporated lignin-capped silver nanoparticles for chronic wound treatment. Ind Eng Chem Res 2020;59:4504–4514.
20. Chaerunnisa A, Madhuvu A, Najm D, Fooladi E, Team V. Effectiveness and safety of different dressing and securement methods for peripheral intravenous catheters: A systematic review and meta-analysis. Int Wound J 2026;23:e70875.
21. Ho CY, Chou HY, Wang SH, Lan CY, Shyu VBH, Chen CH, *et al*. A comprehensive analysis of moist versus non-moist dressings for split-thickness skin graft donor sites: A systematic review and meta-analysis. Health Sci Rep 2025;8:e70315.
22. Bruckner-Tuderman L, Mellerio J. Wound healing in epidermolysis bullosa. British J Dermatol 2017;177:e193–e195.
23. Vlassov S, Oras S, Antsov M, Sosnin I, Polyakov B, Shutka A, *et al*. Adhesion and mechanical properties of PDMS-based materials probed with AFM: A review. Rev Adv Mater Sci 2018;56:62–78.
24. Su L-Y, Yao M, Xu W, Zhong M, Cao Y, Zhou H. Cascade encapsulation of antimicrobial peptides, exosomes and antibiotics in fibrin-gel for first-aid hemostasis and infected wound healing. Int J Biol Macromol2024;269:132140.
25. Mohammadi A, Goneirani ZS, Fatahi A. A review on chitosan-containing polyurethanes: Synthesis, properties and applications. Iran J Polym Sci Technol 2023;36:3–22.
26. Sadeghi S, Bakhshandeh H, Ahangari Cohan R, Peirovi A, Ehsani P, Norouzian D. Synergistic anti-Staphylococcal activity of niosomal recombinant lysostaphin-LL-37. Int J Nanomedicine 2019:9777–9792.
27. Tokumaru S, Sayama K, Shirakata Y, Komatsuzawa H, Ouhara K, Hanakawa Y, *et al*. Induction of keratinocyte migration via transactivation of the epidermal growth factor receptor by the antimicrobial peptide LL-37. J Immunol 2005;175:4662–4668.
28. Jastrzebska E, Zakrzewska A, Flis S, Sokolowska P, Bulka M, Dybko A, *et al*. Biological characterization of the modified poly (dimethylsiloxane) surfaces based on cell attachment and toxicity assays. Biomicrofluidics 2018;12: 044105.
29. Fahimirad S, Khaki M, Ghaznavi-Rad E, Abtahi H. Investigation of a novel bilayered PACL/PVA electrospun nanofiber incorporated Chitosan-LL37 and Chitosan-VEGF nanoparticles as an advanced antibacterial cell growth-promoting wound dressing. Int J Pharm 2024:124341.
30. Samavati SS, Kashanian S, Derakhshankhah H, Abuzade RA, Sajadimajd S, Rabiei M. Pcl and pcl-jaft nanofiber, synthesis, characterization, and histological comparison of the quality of wound healing. J Drug Deliv Sci Technol 2023;84:104457.
31. Park HJ, Cho DH, Kim HJ, Lee JY, Cho BK, Bang SI, *et al*. Collagen synthesis is suppressed in dermal fibroblasts by the human antimicrobial peptide LL-37. J Invest Dermatol 2009;129:843–850.
32. Dal Pra I, Petrini P, Charini A, Bozzini S, Farè S, Armato U. Silk fibroin-coated three-dimensional polyurethane scaffolds for tissue engineering: interactions with normal human fibroblasts. Tissue Eng 2003;9:1113–1121.
33. Esteban-Vives R, Young MT, Ziembicki J, Corcos A, Gerlach JC. Effects of wound dressings on cultured primary keratinocytes. Burns 2016;42:81–90.
34. Liang Y, Wang J, Liu X, Chen S, He G, Fang X, *et al*. Anti-adhesion multifunctional poly (lactic-co-glycolic acid)/ polydimethylsiloxane wound dressing for bacterial infection monitoring and photodynamic antimicrobial therapy. Int J Biol Macromol 2024;260:129501.
35. Chen B, He B, Tucker AM, Biluck I, Leung TH, Schaer TP, *et al*. An environmentally stable, biocompatible, and multilayered wound dressing film with reversible and strong adhesion. Adv Healthc Mater 2024:2400827.
36. Huang C, Wu Q, Li X, Pan P, Gu S, Tang T, *et al*. Silicone bioadhesive with shear-stiffening effect: Rate-responsive adhesion behavior and wound dressing application. Biomacromolecules 2024; 25:4510-4522.